IEEE Access
Multidisciplinary | Rapid Review | Open Access Journal

Received December 21, 2018, accepted January 14, 2019, date of publication January 25, 2019, date of current version March 25, 2019.

Digital Object Identifier 10.1109/ACCESS.2019.2895062

New Rapid and Robust Color Image Watermarking Technique in Spatial Domain

QINGTANG SU[1], DECHENG LIU[1], ZIHAN YUAN[1], GANG WANG[1], XIAOFENG ZHANG[1], BEIJING CHEN[2], AND TAO YAO[1]

[1]School of Information and Electrical Engineering, Ludong University, Yantai 264025, China
[2]Jiangsu Engineering Center of Network Monitoring, School of Computer & Software, Nanjing University of Information Science and Technology, Nanjing 210044, China

Corresponding author: Qingtang Su (sdytsqt@163.com)

This work was supported in part by the Natural Science Foundation of China under Grant 61771231, in part by the Natural Science Foundation of Shandong Province under Grant ZR2017MF010, in part by the Natural Science Foundation of China under Grant 61772253, Grant 61873117, and Grant61872170, and in part by the Natural Science Foundation of Shandong Province under Grant ZR2016FM21, Grant ZR2016FM13, and Grant ZR2017MF062.

ABSTRACT In this paper, a novel spatial domain color image watermarking technique is proposed to rapidly and effectively protect the copyright of the color image. First, the direct current (DC) coefficient of 2D-DFT obtained in the spatial domain is discussed, and the relationship between the change of each pixel in the spatial domain and the change of the DC coefficient in the Fourier transform is proved. Then, the DC coefficient is used to embed and extract watermark in the spatial domain by the proposed quantization technique. The novelties of this paper include three points: 1) the DC coefficient of 2D-DFT is obtained in the spatial domain without of the true 2D-DFT; 2) the relationship between the change of each pixel in the image block and the change of the DC coefficient of 2D-DFT is found, and; 3) the proposed method has the short running time and strong robustness. The experimental results on two publicly available image databases (CVG-UGR and USC-SIPI) have shown that the proposed method not only has satisfied the needs of invisibility but also has better performance in terms of robustness and real-time feature, which show the proposed method has both advantages of spatial domain and frequency domain.

INDEX TERMS Watermarking, DC coefficient, spatial domain, color image, discrete Fourier transform.

I. INTRODUCTION

The protection of multimedia copyright has attracted a lot of attention during the last two decades, and how to rapidly and effectively protect the copyright is an urgent problem. In the context of digital products, digital watermarking has been considered as a suitable solution for protecting copyright [1]–[4]. Digital watermarking technique is the procedure of embedding a small signal called ''watermark'' into the digital product (such as audio, image, video, text etc.), and the watermark can be detected or extracted later by computing operations in order to make assertions about the digital product. The watermark is hidden in the host data in such a way that it is inseparable from the host data and so that it is resistant to many hostile operations.

Based on the differences between processing domains, watermarking method has two types: spatial domain watermarking method and frequency domain watermarking method. For the spatial domain image watermarking technique, the watermark is directly embedded by modifying the pixel values or using the least significant bit (LSB) of the original image. For instance, Sharma *et al.* [5] used the LSB technique to embed watermark image in an original image since it had less impact on the image perceptibility. They also used multiple-parameter discrete fractional Fourier transform (MPDFRFT) with random DFRFT to improve the robustness; hence, this method was dual domain method, and its running time was very long. Chou and Wu [6] proposed a color image watermarking technique in the spatial domain, where the color watermark was embedded into each color pixel by quantization technique. Although this method was spatial domain technique, it needed more time since the forward transform and inverse transform between RGB color space and CIE-Lab color space were needed in the watermarking procedures. Moreover, the experimental results showed that its robustness was weak. Generally, the single

The associate editor coordinating the review of this manuscript and approving it for publication was Zhaoqing Pan.

spatial watermarking method has good real-time feature, but its robustness is relatively weaker than other frequency watermarking methods.

For the frequency domain image watermarking technique, the carrier image is transformed into frequency domain and the watermark information is embedded into the frequency coefficient, which improves the robustness but increases the running time of watermarking method. When a watermark is embedded in the frequency domain, its energy is spread throughout the carrier image by strongly embedding in the host image with less distortion. Thus, these algorithms are robust in preserving watermarks even if the watermarked images are damaged by the potential attacks [7]. For example, Cedillo-Hernandez *et al.* [8] proposed a robust watermarking method in discrete Fourier transform (DFT) domain for effective management of medical imaging. In [8], the embedding process was done in about 8.89 seconds, while the detection process was about 5.87 seconds. Aherrahrou and Tairi [9] proposed DFT watermarking methods to enhance the robustness since DFT can resist geometric attacks and the distribution of energy. Urvoy *et al.* [10] proposed a novel DFT watermarking scheme featuring perceptually optimal visibility versus robustness, and this proposed approach had high robustness to various kinds of attacks. At the same times, some robust watermarking techniques against desynchronization attacks have been surveyed and presented. For example, Licks and Jordan [23] described the most common types of geometric attacks and surveyed the existing solutions. Tian *et al.* [24] presented a blind image watermarking resynchronization scheme against local transform attacks. They used the local daisy feature transform and the binary space partitioning tree to embed watermark information. In general, the frequency domain method has strong robustness but it takes more time.

How to make full use the advantages of frequency domain in spatial domain is still an important science problem. Based on the generating procedure of the direct current (DC) coefficient in discrete Cosine transform (DCT) domain and its distributing feature, an amalgamation domain watermarking method was realized in the spatial domain [11]. The experimental results showed that the method [11] not only had strong robustness but also had lower computation complexity. However, the binary image was used as watermark image in [11], that is, it could not be directly used to embed the 24-bit color image watermark into color host image because its embedding capacity was small.

With the rapid development of digital products, the color images have become the main digital products, and some color image watermarking methods have been proposed and performed in spatial domain or frequency domain. At present, only a few of image watermarking methods in spatial domain using color image as watermark were proposed. For example, Chou and Wu [6] proposed the spatial domain color image watermarking method. But, many image watermarking methods used color image as watermark have been proposed in frequency domain. For instance, Golea *et al.* [12] proposed a blind color image watermarking based on singular value decomposition (SVD). In [12], the singular values were modified for embedding watermark, which results in the watermarked image was seriously distorted since some singular values had been changed. Based on the feature of Schur decomposition, Su *et al.* [13] proposed a blind color image watermarking scheme, which needed to enhance the invisibility. Jia proposed a novel color image watermarking algorithm based on SVD decomposition for protecting the copyright of color image [14]. In [14], the similar relationship of elements in U matrix after SVD was found and used to extract the embedded watermark without resorting to the original data, but its computation complexity was high because the SVD and the inverse SVD with computation complexity $O(n^3)$ were needed in this method. In our previous work [15], a new color watermarking schemes based on LU decomposition was proposed to protect the copyright of color image, which has strong robustness. The methods [20] and [21] all used QR decomposition to embed watermark information into color image; but, the method [21] used the binary image as watermark and it could not be extended to embed color image of sized 32×32 into host color image of sized 512×512. These above-mentioned color watermarking methods are summarized by Table 1.

TABLE 1. The performance of the related methods.

Method	Processing domain	Invisibility	Robustness	Real-time
Method [5]	Dual domain	√	√	×
Method [6]	Spatial	√	×	×
Method [7]	Frequency	√	×	×
Method [8]	Frequency	×	√	×
Method [9]	Frequency	×	√	×
Method [10]	Frequency	√	√	×
Method [11]	Spatial	√	√	√
Method [12]	Frequency	×	√	×
Method [13]	Frequency	×	√	×
Method [14]	Frequency	×	√	×
Method [15]	Frequency	√	√	×
Method [20]	Frequency	√	√	√
Method [21]	Frequency	√	√	√
Method [24]	Frequency	√	√	×

In this paper, a rapid and robust blind watermarking technique in spatial domain is proposed and investigated. Firstly, the method of obtaining the DC coefficient of 2D-DFT in the spatial domain is discussed, and then the rule of distributing the changed quantity of DC coefficient in the spatial domain is further researched and proved. Based on the features of the DC coefficient of 2D-DFT, the novel spatial watermarking method is designed to embed color watermark image into color carrier image and extract the embedded watermark without the help of original color watermark image or original color host image. The results of experiment show that the proposed method has stronger robustness than the existing

spatial domain methods and lower running time than the existing frequency domain methods. The novelties of this paper include three points: (i) the DC coefficient of 2D-DFT is obtained in the spatial domain without of the true 2D-DFT; (ii) the relationship between the change of each pixel in the image block and the change of the DC coefficient of 2D-DFT is proved; (iii) the proposed method has the short running time and strong robustness.

The rest of the paper is organized as follows. In Section II, the preliminaries of discrete Fourier transform and Arnold transform are introduced. Section III discusses the special feature of the DC coefficient of 2D-DFT. Section IV gives the detailed procedures of the proposed watermarking technique. Section V shows the performance evaluation and analysis. At last, the conclusions are drawn in Section VI.

II. PRELIMINARIES

As an important technique of frequency domain, DFT is often used in frequency domain analysis. Hence, it is necessary to know the special feature of DFT in the spatial domain. In addition, the security of watermarking is ensured by many techniques, where the Arnold transform is often used to permute the watermark image

A. DISCRETE FOURIER TRANSFORM

The Fourier transform is the most basic transform. Many problems can be processed in the spatial domain and transform domain with DFT at the same time. The DFT can be used to represent the discrete information since the image is stored in computer with digital form. The 2D-DFT and 2D-inverse DFT (2D-IDFT) are introduced as follows.

If the two-dimensional function $f(x, y)$ satisfies the Dirichlet conditions: (i) it has finite discontinuous points, (ii) it has finite poles, and (iii) it is absolutely integrable, then the 2D-DFT can be denoted by

$$\mathcal{F}(u, v) = \sum_{x=0}^{M-1} \sum_{y=0}^{N-1} f(x, y) \mathrm{e}^{-j2\pi xu/M} \mathrm{e}^{-j2\pi yv/N}, \quad (1)$$

where, x, y are the variables of spatial frequency, $x = 0, 1, \ldots, M-1$, $y = 0, 12, \ldots, N-1$, u, v are the variables of transform frequency, $u = 0, 1, \ldots, M-1$, $v = 0, 12, \ldots, N-1$, M and N are the sizes of the image in the direction of width and height, and $\mathcal{F}(u, v)$ is called the DFT coefficient of function $f(x, y)$.

The 2D-IDFT is denoted by

$$f(x, y) = \frac{1}{MN} \sum_{u=0}^{M-1} \sum_{v=0}^{N-1} \mathcal{F}(u, v) \mathrm{e}^{j2\pi xu/M} \mathrm{e}^{j2\pi yv/N}, \quad (2)$$

where $x = 0, 1, \ldots, M-1$; $y = 0, 1, \ldots, N-1$.

According to (1), when $u = 0$ and $v = 0$, the direct current (DC) coefficient $\mathcal{F}(0, 0)$ can be calculated by

$$\mathcal{F}(0, 0) = \sum_{x=0}^{M-1} \sum_{y=0}^{N-1} f(x, y). \quad (3)$$

It is known from (3) that the DC coefficient of image block can be directly obtained in the spatial domain.

According to (2), the inverse transform of (3) can be obtained by

$$f(x, y) = \frac{1}{MN} \mathcal{F}(0, 0). \quad (4)$$

Suppose the watermarked result is $\mathcal{F}(0, 0)'$ when the watermark is embedded into DC coefficient $\mathcal{F}(0, 0)$, then the watermarked $f(x, y)'$ in the spatial domain is gotten by

$$f(x, y)' = \frac{1}{MN} \mathcal{F}(0, 0)', \quad (5)$$

The changed quantity $\Delta f(x, y)$ in spatial domain of each watermarked pixel is gotten by

$$\Delta f(x, y) = f(x, y)' - f(x, y) = \frac{1}{MN} (\mathcal{F}(0, 0)' - \mathcal{F}(0, 0)). \quad (6)$$

It can be seen from (6) that the change quantity of each pixel in the image block depends on the change quantity of the DC coefficient of the Fourier transform. Hence, the process of using the DC coefficient to embed watermark by the Fourier transform can be instead by modifying the pixel value in the spatial domain. This feature has been used to image compression storage. In this paper, we will extend this feature to image watermarking field. This is one of the significant novelties of this work.

B. ARNOLD TRANSFORM

Since Arnold transform has high efficiency, it has been widely used to permute watermark image for watermark security [4]. The detailed definition of Arnold transform is given by

$$\begin{bmatrix} i' \\ j' \end{bmatrix} = \mathrm{mod} \left(\begin{bmatrix} 1 & 1 \\ 1 & 2 \end{bmatrix} \begin{bmatrix} i \\ j \end{bmatrix}, M \right), \quad (7)$$

where i, j, i' and j' are four integers in $\{0, 1, 2, \ldots, M-1\}$, M is the size of square image matrix, mod(.) is the standard modular function, i and j are the pixel position in the original image matrix, and i' and j' are the new pixel position in the transformed image matrix. That is, the pixel at the position (i, j) of original image matrix will be transformed to a new position (i', j') by (7), which will change the order of matrix pixels and enhances the security in visual identification of watermark image. Moreover, the iteration number of Arnold transform is used as the secret key.

When restoring the original image matrix, the corresponding inverse procedure of Arnold transform can be defined by

$$\begin{bmatrix} i \\ j \end{bmatrix} = \mathrm{mod} \left(\begin{bmatrix} 2 & -1 \\ -1 & 1 \end{bmatrix} \begin{bmatrix} i' \\ j' \end{bmatrix}, M \right). \quad (8)$$

C. HASH PSEUDORANDOM SCRAMBLING ALGORITHM

For ensuring the security of watermarking method, the so-called Hash pseudorandom scrambling algorithm based on the Hash function is used to randomly select the non-collision embedding blocks in this paper. Hash function is an important

basic tool in the field of information security, and it is widely used in the fields of public key cryptography, digital signatures, integrity, and authentication [19].

Hash function mainly includes two types: MDx and SHAx, in which MD5 algorithm is the representative of MD type. The principle of MD5 is described as follows: The inputted information is processed by MD5 algorithm with the group of size 512 bits, and each group is further divided sixteen sub-groups of size 32 bits. Four registers are used in the MD5 algorithm, and four-turn compress algorithm is beginning when the values of four registers are initialized. In the process of four-turn compress, their operation structures are same, but their Boolean functions, definite value parameters and the bits of cyclic shift to the left are different. There are sixteen iterations in each turn, that is, four turns include 64 iterations. After the compression of four turns, the corresponding values of each register are obtained and added to one information digest of size 128 bits.

III. THE PROPOSED METHOD

In this paper, both the original host image and the watermark image are 24-bits color images. The overall watermarking technique includes two processes: embedding watermark and extracting watermark. Each process is explained in detail as follows, respectively.

A. EMBEDDING WATERMARK

In this process, the decimal format of color watermark image will be transformed to binary format, and one bit watermark information will be embedded into one image blocks of sized 4×4. As shown in Fig.1, the process of embedding watermark includes many steps. For clarity, the detailed steps are descried as follows.

Step 1: Pre-processing the host image and watermark image.

Firstly, one 24-bit color host image H with size of $M \times M$ is divided into red, green and blue three color channels, every color channel is divided into non-overlapping pixel blocks with size of $m \times m$, where $m = 4$.

Secondly, one 24-bit color watermark image W with size of $N \times N$ is divided into red, green and blue three color channels. Each color channel watermark W_i is permutated by Arnold transform based on key Ka_i in order of red, green and blue. In here, the key Ka_i is selected by the period of the Arnold transform, and the transform period is determined by the matrix size [21]. The decimal format of each pixel value of each color channel watermark is transformed to 8 bits binary format. The binary values in the channel watermark W_i are linked to the watermark string sequence SW_i. The length of sequence SW_i is $N \times N \times 8$, where $i = 1, 2, 3$, and represents three color channels of red, green and blue, respectively. Since one watermark information is embedded into one image block of sized 4×4, i.e. $(M \times M)/(N \times N \times 8) \geq (4 \times 4)$, so the size of host image and the size of watermark image should meet $M \geq 8\sqrt{2}\,N$.

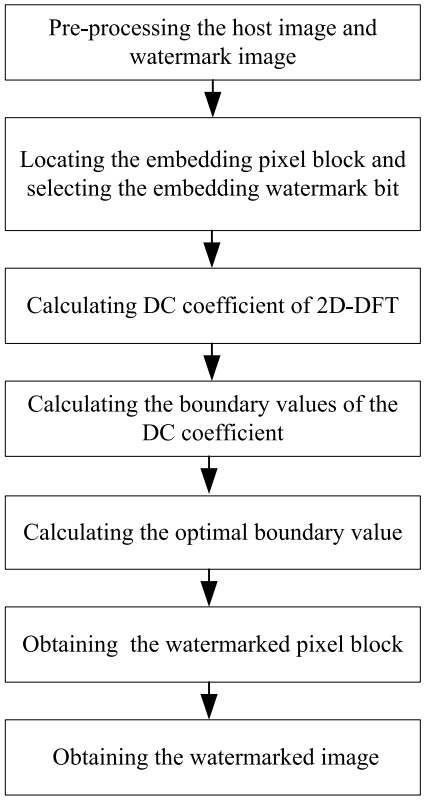

FIGURE 1. The flowchart of embedding watermark.

Step 2: Locating the embedding pixel block and selecting the embedding watermark bit.

Embedding pixel block BK is located by using the localization matrix which is generated by Hash pseudo-random scrambling algorithm based on key Kb_i. At the same time, the embedding watermark bit w is selected from the binary string sequence SW_i of the corresponding channel, where $i = 1, 2, 3$, and represents three color channels of red, green and blue, respectively.

Step 3: Calculating the DC coefficient of 2D-DFT.

Using (9) to obtain the DC coefficient DCC of embedding pixel blockBK in the spatial domain, which does not need the true 2D-DFT transform and can decrease the execution time.

$$DCC = \sum_{p=1}^{m} \sum_{q=1}^{m} BK(p, q), \tag{9}$$

where $BK(p, q)$ represents the pixel value at the coordinate (p, q) in the embedding pixel block BK, p and q are more than 1 and less than m, and m is the width (or height) of the embedding pixel block BK.

Step 4: Calculating the boundary values of the DC coefficient.

In the proposed method, the quantization technique is used to embed watermark. Any value will be located between two quantization boundary values. The lower boundary value C_{low} and upper boundary value C_{high} of DC coefficient DCC are

calculated by (10) and (11).

$$C_{low} = \begin{cases} floor(DCC/T) \times T + 0.25 \times T, & if\ w =' 1 \\ (floor(DCC/T) - 1) \times T + 0.75 \times T, & if\ w = '0', \end{cases} \tag{10}$$

$$C_{high} = \begin{cases} (floor(DCC/T) + 1) \times T + 0.25 \times T, & if\ w = '1' \\ floor(DCC/T) \times T + 0.75 \times T, & if\ w = '0', \end{cases} \tag{11}$$

where w is the embedding watermark bit, $floor(.)$ is the downward integral function, and T is the quantization step.

Step 5: Calculating the optimal boundary value.

According to (12), the optimal boundary value OC is selected from the upper boundary values C_{high} or lower boundary values C_{low}.

$$OC = \begin{cases} C_{low}, & if\ abs(C_{low} - DCC) \le abs(C_{high} - DCC) \\ C_{high}, & else, \end{cases} \tag{12}$$

where abs (.) is absolute value function.

Step 6: Calculating the watermarked pixel block.

Using (13) to distribute the changed quantity CHC of DC coefficient to all pixels of the pixel block BK evenly, then the watermarked pixel blocks BK^* are obtained. The embedding pixel block in the corresponding color channel is replaced with the watermarked pixel block.

$$BK^* = BK + CHC/(m \times m), \tag{13}$$

where $CHC = OC\text{-}DCC$, m is the width (or height) of the embedding pixel block. This method can reduce the execution time without the 2D-IDFT.

Step 7: Repetitive execution.

Repeating the steps 2 to 6 until all the watermark bits are embedded into three color channels. Finally, recombining the red, green and blue color channels to obtain the watermarked image H^*.

B. EXTRACTING WATERMARK

In this process, the embedded watermark information will be extracted from the final watermarked image H^*. As shown in Fig. 2, the process of extracting watermark is the inverse process of embedding watermark, and its detailed steps are given as follows.

Step 1: Pre-processing the watermarked image H^*.

The watermarked image H^* is divided into red, green and blue three color channels H_i^*, where $i = 1, 2, 3$, and represents three color channels of red, green and blue, respectively. Each color channel is divided into non-overlapping pixel blocks of sized $m \times m$.

Step 2: Locating watermarked pixel block.

The watermarked pixel block BK^* is selected by the Hash pseudo-random scrambling algorithm based on key Kb_i,

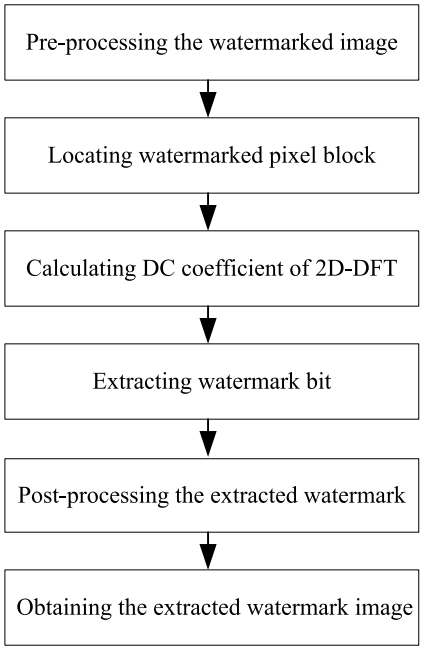

FIGURE 2. The flowchart of extracting watermark.

where $i = 1, 2, 3$, and represents three color channels of red, green and blue, respectively.

Step 3: Calculating the DC coefficient of 2D-DFT.

The DC coefficient DCC^* of the watermarked pixel block BK^* is directly obtained from (14), and the acquisition of DC coefficient does not need the true 2D-DFT transform.

$$DCC^* = \sum_{p=1}^{m} \sum_{q=1}^{m} BK^*(p, q), \tag{14}$$

where $BK^*(p, q)$ represents the pixel value at the coordinate (p, q) in the watermarked pixel block BK^*, p and q are more than 1 but less than m, and m is the width (or height) of the watermarked pixel block BK^*.

Step 4: Extracting watermark bit.

The watermark bit w is extracted by (15), where $mod(\ )$ is the modular function and $round(\ )$ is the rounding function.

$$w = \begin{cases} '1', & if\ mod(round(DCC^*), T) < 0.5 \times T \\ '0', & else, \end{cases} \tag{15}$$

Step 5: Repetitive execution.

The above Steps 2-4 are repeated, and all extracted watermark bits are linked to the binary string sequence SW_i^* of each channel respectively. Then, SW_i^* is converted to decimal pixel values in a set of 8-bit binary strings, where $i = 1, 2, 3$, and represents three color channels of red, green and blue, respectively.

Step 6: Post-processing the extracted watermark.

Performing inverse Arnold transform with key Ka_i on the decimal pixel values of each channel. Then, the extracted watermark component W_i^* of each channel is obtained, where

$i = 1, 2, 3$, and represents three color channels of red, green and blue, respectively.

Step 7: Recombining the extracted watermark component.

The extracted watermark component W_i^* of each channel is reconstructed to obtain the extracted 24-bit color watermark image W^*.

IV. PERFORMANCE EVALUATION AND ANALYSIS

In order to fairly and accurately evaluate watermarking performance in terms of invisibility, robustness and real-time feature, it is necessary to do some simulations and compare the proposed method to some related color image watermarking methods. Hence, the test images and metrics should be approved by many watermarking researchers.

A. DATASET

In this study, all color images of the databases CVG-UGR [17] and USC-SIPI [18] are used as the host images to test the performance of this method. All host images are 24 bits/pixel for color images, and each host image is resized to 512 × 512 pixels.

For showing the performance of this method, ten original images are selected from the databases and used as color host images to compare with the state-of-the-art methods [12]–[16]. As shown in Fig. 3, all of the 24-bits color images have the same size, i.e. 512×512. Furthermore, all of the 24-bits color watermark images have also the same size, i.e. 32×32, as shown in Fig. 4. These watermark images have been used in other compared methods [12]–[16].

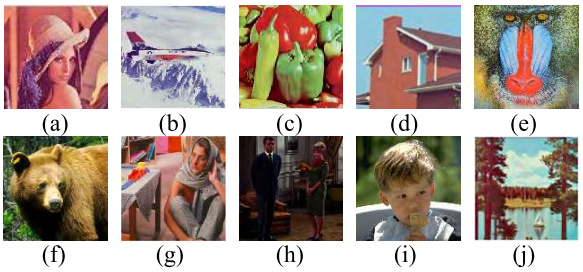

FIGURE 3. Host images: (a) Lena, (b) Avion, (c) Peppers, (d) House, (e) Baboon, (f) Bear, (g) Barbara, (h) Couple, (i) Kid, and (j) SailBoat.

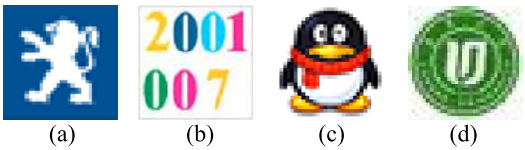

FIGURE 4. Watermark images: (a) Watermark image 1, (b) Watermark image 2, (c) Watermark image 3, and (d) Watermark image 4.

B. METRICS

In this experiment, the traditional method Peak Signal-to-Noise Ratio (PSNR), as shown by (16), is used to compute the similarity between the original color image H and the watermarked image H^* [20]

$$PSNR = (\sum_{j=1}^{3} PSNR_j)/3, \tag{16}$$

where $PSNR_j$ denotes the PSNR of their red, green and blue channels, $j = \{1, 2, 3\}$, respectively,

$$PSNR_j = 10 \lg \frac{M \times N \times \max\{[H(x, y, j)]^2\}}{\sum_{x=1}^{M} \sum_{y=1}^{N} [H(x, y, j) - H^*(x, y, j)]^2}, \tag{17}$$

where $H(x, y, j), H^*(x, y, j)$ stands for the value of pixel (x, y) in channel j of the original image and the watermarked one, and M, N denotes the width and height of the host images, respectively.

In addition, the Structural Similarity Index Measurement (SSIM), as denoted by (18), is also used to compute the similarity between the original color image H and the watermarked image H^*.

$$SSIM(H, H^*) = l(H, H^*)c(H, H^*)s(H, H^*), \tag{18}$$

where

$$\begin{cases} l(H, H^*) = (2\mu_H \mu_{H^*} + C_1)/(\mu_H^2 + \mu_{H^*}^2 + C_1) \\ c(H, H^*) = (2\sigma_H \sigma_{H^*} + C_2)/(\sigma_H^2 + \sigma_{H^*}^2 + C_2) \\ s(H, H^*) = (\sigma_{HH^*} + C_3)/(\sigma_H \sigma_{H^*} + C_3), \end{cases} \tag{19}$$

the first term in (19) is the luminance comparison function which measures the closeness of the two images' mean luminance (μ_H and μ_{H^*}). The second term is the contrast comparison function which measures the closeness of the contrast of the two images. Here the contrast is measured by the standard deviation σ_H and σ_{H^*}. The third term is the structure comparison function which measures the correlation coefficient between the two images H and H^*. Note that σ_{HH^*} is the covariance between H and H^*. The positive values of the SSIM index are in [0, 1]. A value of 0 means no correlation between images, and 1 means that $H = H^*$. The positive constants C_1, C_2 and C_3 are used to avoid a null denominator.

Besides, in order to measure the robustness of the watermark, Normalized Cross-correlation (NC) between the original watermark W and the extracted watermark W^* is used and shown as follows.

$$NC = \frac{\sum_{i=1}^{3} \sum_{x=1}^{P} \sum_{y=1}^{Q} (W(x, y, j) \times W^*(x, y, j))}{\sqrt{\sum_{j=1}^{3} \sum_{x=1}^{P} \sum_{y=1}^{Q} [W(x, y, j)]^2} \sqrt{\sum_{j=1}^{3} \sum_{x=1}^{P} \sum_{y=1}^{Q} [W^*(x, y, j)]^2}} \tag{20}$$

where the P and Q denote the row and column size of the original watermark image.

For selecting the effective quantization step, we do many experiments at first. Fig. 5 gives the different results of invisibility and robustness under different quantization steps.

TABLE 2. THE invisibility results (PSNR/SSIM) when embedding test watermark image 1 into host images.

	Watermark1	Watermark2	Watermark3	Watermark4
Lena	38.0535/0.9414	37.9574/0.9409	38.0103/0.9409	38.0357/0.9412
Avion	38.1039/0.9353	37.7578/0.9305	37.8693/0.9316	38.0165/0.9339
Peppers	37.6262/0.9231	37.8108/0.9274	37.7327/0.9251	37.6172/0.9233
House	37.8923/0.9233	37.7408/0.9238	37.7080/0.9212	37.8697/0.9233
Baboon	37.9085/0.9794	37.8179/0.9787	37.8455/0.9787	37.8196/0.9788
Bear	36.8809/0.9250	37.3998/0.9358	37.2199/0.9318	36.9836/0.9273
Barbara	37.8867/0.9461	38.0469/0.9500	37.9500/0.9478	37.9241/0.9470
Couple	36.5176/0.8909	37.5593/0.9143	37.1916/0.9058	36.9142/0.8997
Kid	37.2256/0.9241	36.8341/0.9230	37.9486/0.9226	36.9878/0.9222
Baboon	37.6931/0.9433	37.7440/0.9458	36.6796/0.9440	37.7076/0.9438
Average	37.5788/0.9332	37.6659/0.9370	37.6155/0.9350	37.5876/0.9340

TABLE 3. The comparison of PSNR and SSIM of variouos watermarking mothods.

Image	Method [12]	Method [13]	Method [14]	Method [15]	Method [16]	Method [20]	Proposed method
Lena	39.4358/0.9935	39.4358/0.9777	38.3965/0.9668	39.4428/0.9816	22.5616/0.6332	35.3414/0.9717	38.0535/0.9414
Avion	38.3922/0.9540	38.3922/0.9651	35.3004/0.9954	36.6958/0.9675	20.4106/0.5411	32.4966/0.9447	38.1039/0.9353
Peppers	34.4587/0.9279	35.8301/0.9671	38.9360/0.9773	40.8216/0.9878	23.2864/0.7111	36.4253/0.9783	37.6262/0.9231
House	34.4806/0.9970	34.4642/0.9454	37.0763/0.9504	40.1223/0.9793	25.6319/0.9249	35.7681/0.9622	37.8923/0.9233

When the quantization step T is increased, the invisibility of watermarking method is decreased since the host image will be modified with a great quantity. In general, the robustness is increased with the increased quantization step T. It can be seen from the Fig 5, the quantization step T is selected to be 125 in this experiment considering the trade-off between the invisibility and robustness.

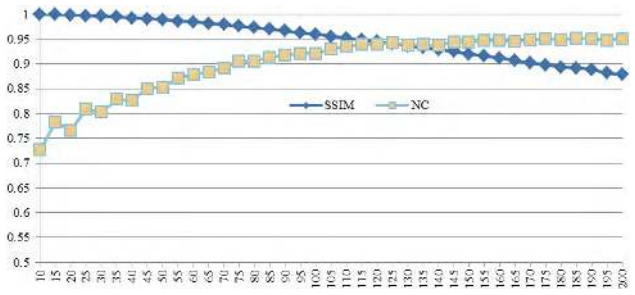

FIGURE 5. The different results of invisibility and robustness under different quantization steps.

C. INVISIBILITY TEST AND ANALYSIS

The watermark invisibility is one of the most important features of watermarking. For the invisible watermarking method, the embedded watermark should be imperceptible. Only if the embedded watermark cannot be noticed in vision and it can be whole extracted from the watermarked image, then the other features can be further meaning discussed.

For showing the invisibility of the proposed method when the watermark image extracted from the watermarked image with free-attack is the same as the original watermark image, four different watermark images are embedded into all host images, and part of results are given in Table 2. When the 32×32 color watermark images are embedded into the given host images, their average PSNR values are more than 35dB, and their average SSIM values are near to 1. There is very little difference between these values for the ten test images with the quantization step 125, which shown the proposed method has good and stable imperceptibility of watermark. In a word, the imperceptibility is mainly determined by the quantization step mentioned in the above sub-section.

For fair comparison and succinct presentation, the watermark image 1 is embedded into the four test images used in other related methods. As seen from the Table3, the PSNR values of the proposed method are more than 37dB, and their SSIM values are near to 1, which indicates that the difference between the original images and the watermarked images cannot be distinguished by human eyes. Hence, the proposed method is effective to embed watermark. Although the method [16] can be extended to use color image as watermark image, the effective of invisibility cannot meet the need of color image watermarking. Hence, the method [16] is not compared in the following test.

D. ROBUSTNESS TEST AND ANALYSIS

The robustness is an important metric for watermarking technique. In this section, in order to show the robustness

of our proposed watermarking method, some basic attacks of standard benchmark Optimark software (such as JPEG, Median, Cropping, and Scaling etc.) are selected to test the robustness of the proposed method. Moreover, other attacks adopted in the related methods (such as Low-pass filtering, Salt & Peppers noising, and Gaussian noising etc.) are also used in this method. Further, after extracting the watermark, the well-known metric NC is used to measure the robustness.

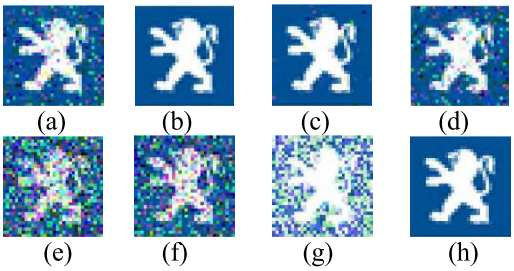

FIGURE 6. Extract the watermark image 1 from the watermarked image "Lena" after different attacks: (a) JPEG (40) NC = 0.9662, (b) JPEG 2000 (5:1) NC = 1.0000, (c) Salt &Peppers noise (0.2%) NC = 0.9990, (d) Gaussian white noise (0, 0.001) NC = 0.9676, (e) Median filtering (3×3) NC = 0.8645, (f) Butterworth low-pass filtering (100, 10) NC = 0.8855, (g) Cropping (50%) NC = 0.8409, and (h) Zoom-in (4:1) NC = 1.0000.

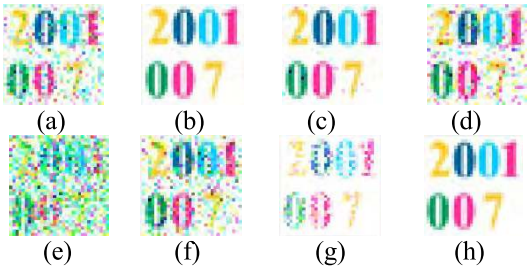

FIGURE 7. Extract the watermark image 2 from the watermarked image "House" after different attacks: (a) JPEG (40) NC = 0.9452, (b) JPEG 2000 (5:1) NC = 1.0000, (c) Salt &Peppers noise (0.2%) NC = 0.9958, (d) Gaussian white noise (0, 0.001) NC = 0.9521, (e) Median filtering (3×3) NC = 0.8413, (f) Butterworth low-pass filtering (100, 10) NC = 0.9144, (g) Cropping (50%) NC = 0.9612, and (h) Zoom-in (4:1) NC = 1.0000.

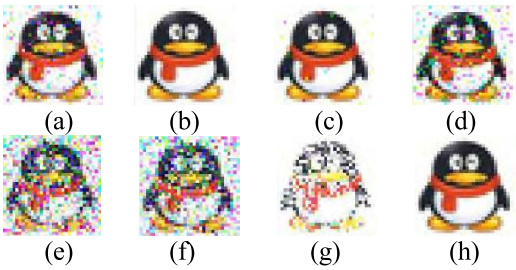

FIGURE 8. Extract the watermark image 3 from the watermarked image "Bear" after different attacks: (a) JPEG (40) NC = 0.9771, (b) JPEG 2000 (5:1) NC = 1.0000, (c) Salt &Peppers noise (0.2%) NC = 0.9956, (d) Gaussian white noise (0, 0.001) NC = 0.8972, (e) Median filtering (3 × 3) NC = 0.8967, (f) Butterworth low-pass filtering (100, 10) NC = 0.8820, (g) Cropping (50%) NC = 0.9236, and (h) Zoom-in (4:1) NC = 1.0000.

For succinct presentation, Figs. 6-9 give the visual effectiveness of extracted different watermarks from the watermarked image "Lena", "House", "Bear", and

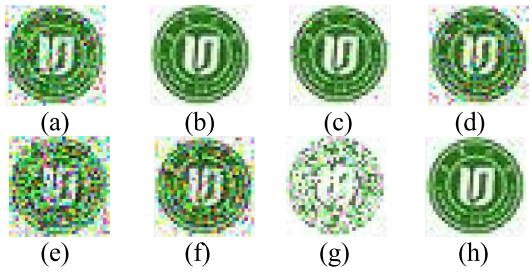

FIGURE 9. Extract the watermark image 4 from the watermarked image "Sailboat" after different attacks: (a) JPEG (40) NC = 0.9598, (b) JPEG 2000 (5:1) NC = 1.0000, (c) Salt &Peppers noise (0.2%) NC = 0.9984, (d) Gaussian white noise (0, 0.001) NC = 0.9712, (e) Median filtering (3 × 3) NC = 0.9088, (f) Butterworth low-pass filtering (100, 10) NC = 0.9508, (g) Cropping (50%) NC = 0.8471, and (h) Zoom-in (4:1) NC = 1.0000.

"Sailboat" after different attacks, respectively. The NC values of Figs. 6(a)-(h) are 0.9662, 1.0000, 0.9990, 0.9676, 0.8645, 0.8855, 0.8409, and 1.0000, the NC values of Figs. 7(a)-(h) are 0.9452, 1.0000, 0.9958, 0.9521, 0.8413, 0.9144, 0.9612, and 1.0000, the NC values of Figs. 8(a)-(h) are 0.9771, 1.0000, 0.9956, 0.8972, 0.8967, 0.8820, 0.9236, and 1.0000, the NC values of Figs. 9(a)-(h) are 0.9598, 1.0000, 0.9984, 0.9712, 0.9088, 0.9508, 0.8471, and 1.0000, respectively. It is seen from these results that the proposed method has strong robustness in most malicious attacks, and these extracted watermark images have good visual quality. Hence, the proposed method can protect the copyright of color image in the most common attacks.

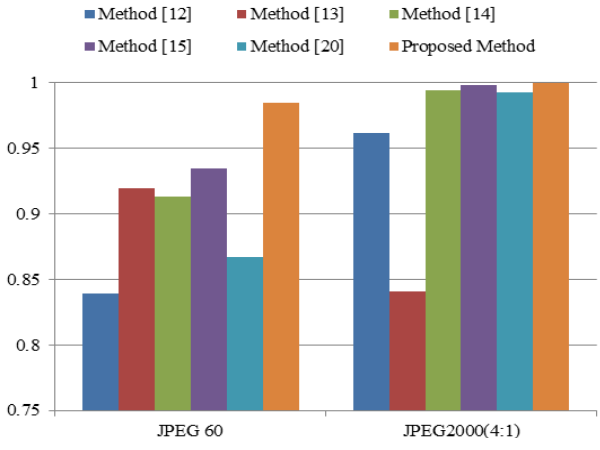

FIGURE 10. The robustness comparison between different methods after image compression attacks.

In order to further demonstrate the robustness of the proposed method, after embedding the watermark image 1 into the test image "Lena", the comparison with other related color image watermarking is presented by Figs. 10-13. At first, Fig. 10 gives the results of against image impression, i.e. JPEG compression with compression factor 60 and JPEG 2000 compression ratio 4:1. Obviously, the robustness of the proposed against image compression is better than other compared methods when the compression parameters

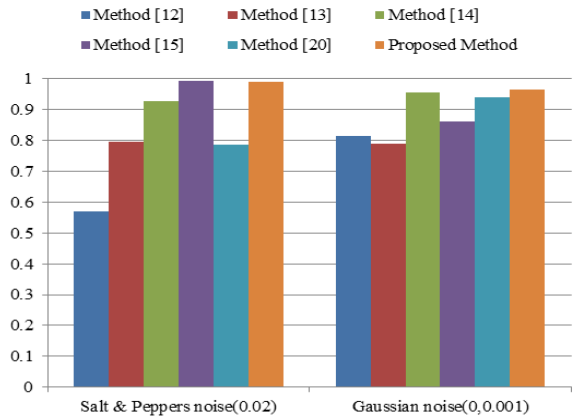

FIGURE 11. The robustness comparison between different methods after noising attacks.

are the same. Then, Fig. 11 illustrates the robustness when adding different noises to the watermarked image. When the Salt &Peppers noise with density 0.02 is added to the watermarked image, the proposed method has better robust than other methods. In addition, the proposed method is strong to resist the attack of adding Gaussian white noise. Furthermore, Fig. 12 gives the results for resisting the different filtering attacks. The first attack is the Butterworth low-pass filtering with cut-off frequency 100 and filter order 10, and the second one is median filtering with window size of 3×3. In general, the proposed method meets the need of the robustness; especially, it has better robust to against the median filtering attack.

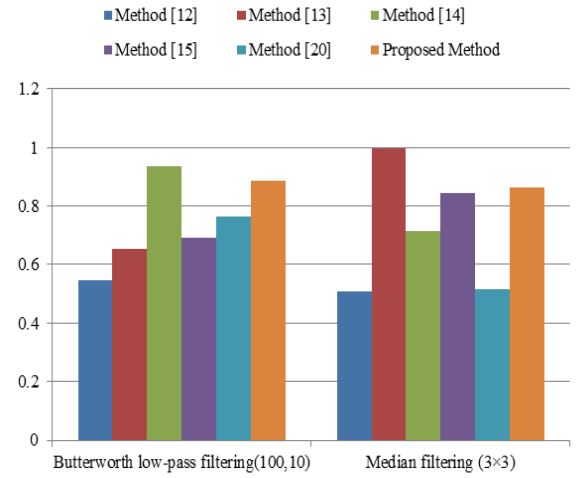

FIGURE 12. The robustness comparison between different methods after filtering attacks.

In addition, Fig. 13 shows the results for resisting the geometric attacks. The first attack is the cropping attack with cropped ratio 50%, and the second one is zooming with 50%. In the cropping attack, the watermarked image is cropped from the left to right with different cropped ratios. In the zooming attack, the watermarked image is zooming out 50% and then resize to the original size, which includes twice zooming operation. As seen from the results, the proposed

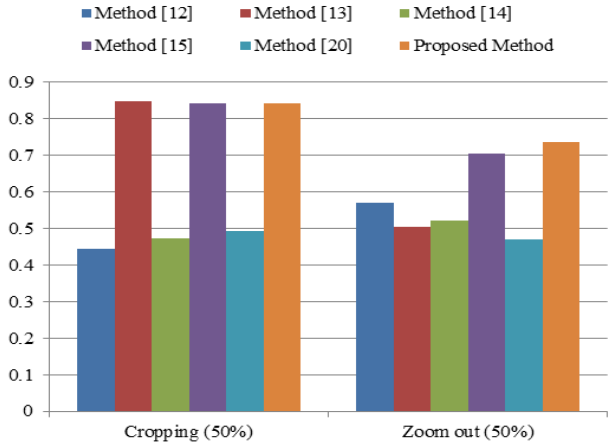

FIGURE 13. The robustness comparison between different methods after cropping and zoom out attacks.

method can resist the common geometric attacks; especially, it has better robustness to against the zooming attack than other compared methods.

Furthermore, an accurate comparison, which is statistical analysis, between our proposed method and other related methods is performed. Accordingly, the statistical significance of the difference between the proposed method and other methods was assessed by the Wilcoxon signed-ranks test with a significance level of 0.05. The Wilcoxon signed-rank test was selected because the results of each attack in both methods did not show normal distribution [25]. This test was performed to compare other methods and the proposed method for each individual type of attack. The NC robustness values against the tested attacks are coming from many experiments.

IBM SPSS statistic 22.0 was used to perform our statistical calculations. In the test, the null hypothesis H_0 indicates that there is no significant difference between the proposed method and other methods. In contrast, the alternative hypothesis H_1 indicates that a significant difference exists between these compared methods. With a 95% confidence level, the null hypothesis H_0 is rejected if $\alpha \leq 0.05$; the null hypothesis H_0 cannot be rejected if $\alpha > 0.05$. In the case of rejecting the null hypothesis H_0 ($\alpha \leq 0.05$), we confirm the critical value for the Wilcoxon signed-rank test w_α^* and the sum of the negative ranks w^- and a decision can be made based on their values [25]. If the sum of the negative ranks value is smaller than the critical value for the Wilcoxon signed-rank test (i.e. $w^- \leq w_\alpha^*$), the proposed method is better than the compared method. Otherwise, the compared method is better [26]. As can be seen from the Table 4, the proposed scheme generally outperforms other schemes in many attacks.

E. REAL-TIME ANALYSIS

In this experiment, all methods are coded in MATLAB 2010a and performed on a laptop computer with Intel Core CPU @ 2.27GHZ and 2G RAM. To compare the computation

TABLE 4. Statistical comparison using the wilcoxon signed-rank testing (the proposed method VS other methods).

	Method [12]	Method [13]	Method [14]	Method [15]	Method [20]
JPEG	Reject H_0, with $\alpha = 0.005, w_\alpha^* = 55, w^- = 0, w^- \le w_\alpha^*$	Reject H_0, with $\alpha = 0.005, w_\alpha^* = 55, w^- = 0, w^- \le w_\alpha^*$	Reject H_0, with $\alpha = 0.007, w_\alpha^* = 54, w^- = 1, w^- \le w_\alpha^*$	Cannot reject H_0, with $\alpha = 0.878$	Reject H_0, with $\alpha = 0.005, w_\alpha^* = 55, w^- = 0, w^- \le w_\alpha^*$
JPEG 2000	Reject H_0, with $\alpha = 0.005, w_\alpha^* = 55, w^- = 0, w^- \le w_\alpha^*$	Reject H_0, with $\alpha = 0.005, w_\alpha^* = 55, w^- = 0, w^- \le w_\alpha^*$	Cannot reject H_0, with $\alpha = 0.646$	Cannot reject H_0, with $\alpha = 0.721$	Reject H_0, with $\alpha = 0.013, w_\alpha^* = 52, w^- = 3, w^- \le w_\alpha^*$
Salt & Peppers noise	Reject H_0, with $\alpha = 0.043, w_\alpha^* = 15, w^- = 0, w^- \le w_\alpha^*$	Reject H_0, with $\alpha = 0.043, w_\alpha^* = 15, w^- = 0, w^- \le w_\alpha^*$	Reject H_0, with $\alpha = 0.043, w_\alpha^* = 15, w^- = 0, w^- \le w_\alpha^*$	Cannot reject H_0, with $\alpha = 0.225$	Reject H_0, with $\alpha = 0.043, w_\alpha^* = 15, w^- = 0, w^- \le w_\alpha^*$
Gaussian noise	Reject H_0, with $\alpha = 0.043, w_\alpha^* = 15, w^- = 0, w^- \le w_\alpha^*$	Reject H_0, with $\alpha = 0.043, w_\alpha^* = 15, w^- = 0, w^- \le w_\alpha^*$	Cannot reject H_0, with $\alpha = 0.5$	Reject H_0, with $\alpha = 0.043, w_\alpha^* = 15, w^- = 0, w^- \le w_\alpha^*$	Reject H_0, with $\alpha = 0.043, w_\alpha^* = 15, w^- = 0, w^- \le w_\alpha^*$
Butterworth Low-pass filtering	Reject H_0, with $\alpha = 0.043, w_\alpha^* = 15, w^- = 0, w^- \le w_\alpha^*$	Cannot reject H_0, with $\alpha = 0.5$	Cannot reject H_0, with $\alpha = 0.686$	Reject H_0, with $\alpha = 0.043, w_\alpha^* = 15, w^- = 0, w^- \le w_\alpha^*$	Cannot reject H_0, with $\alpha = 0.138$
Median filtering	Reject H_0, with $\alpha = 0.043, w_\alpha^* = 15, w^- = 0, w^- \le w_\alpha^*$	Cannot reject H_0, with $\alpha = 0.068$	Cannot reject H_0, with $\alpha = 0.144$	Cannot reject H_0, with $\alpha = 0.225$	Cannot reject H_0, with $\alpha = 0.144$
Cropping	Reject H_0, with $\alpha = 0.043, w_\alpha^* = 15, w^- = 0, w^- \le w_\alpha^*$	Cannot reject H_0, with $\alpha = 0.5$	Cannot reject H_0, with $\alpha = 0.08$	Reject H_0, with $\alpha = 0.043, w_\alpha^* = 15, w^- = 0, w^- \le w_\alpha^*$	Cannot reject H_0, with $\alpha = 0.225$
Zooming	Reject H_0, with $\alpha = 0.043, w_\alpha^* = 15, w^- = 0, w^- \le w_\alpha^*$	Reject H_0, with $\alpha = 0.043, w_\alpha^* = 15, w^- = 0, w^- \le w_\alpha^*$	Reject H_0, with $\alpha = 0.043, w_\alpha^* = 15, w^- = 0, w^- \le w_\alpha^*$	Cannot reject H_0, with $\alpha = 0.08$	Reject H_0, with $\alpha = 0.043, w_\alpha^* = 15, w^- = 0, w^- \le w_\alpha^*$

TABLE 5. The comparison of real-time feature between different methods (second).

Method	Time of watermark embedding	Time of watermark extracting	Total Time
Method [12]	1.909066	0.905951	2.815017
Method [13]	1.263168	0.591873	1.855041
Method [14]	0.979948	0.436173	1.416121
Method [15]	0.810820	0.269506	1.080326
Method [20]	0.546941	0.410019	0.956960
Proposed method	0.383260	0.340666	0.723926

complexity of the different methods, the execution times of different methods are given in Table 5. As can be seen from Table 5, although the proposed spatial-frequency method theoretically uses the element of R matrix of QR decomposition when watermark embedding and watermark extracting, the proposed method has shorter running time than other methods since the proposed method performs on the spatial domain, which only includes the simple algebra operation. Hence, one of the advantages of the proposed method is that it has higher real-time feature, which is more suitable to protect the copyright of color image.

V. CONCLUSION

In this paper, a novel spatial domain color image watermarking technique is proposed for protecting the copyright of color image. Firstly, the DC coefficient of 2D-DFT is obtained in the spatial domain. Then, the distribution rule of DC coefficient is derived. Based on the above feature, the DC coefficient based quantization watermarking technique is proposed to protect the copyright of digital color image. Moreover, the proposed watermarking method belongs to blind watermarking method. The experimental results show that the proposed method not only has met the needs of invisibility, but has better performance in terms of robustness and

real-time features. In future, we will consider how to carry on the popularization and application.

REFERENCES

[1] A. Cedillo-Hernandez, M. Cedillo-Hernandez, M. N. Miyatake, and H. P. Meana, "A spatiotemporal saliency-modulated JND profile applied to video watermarking," *J. Vis. Commun. Image Represent.*, vol. 52, pp. 106–117, Apr. 2018.
[2] N. Sahu, and A. Sur, "SIFT based video watermarking resistant to temporal scaling," *J. Vis. Commun. Image Represent.*, vol. 45, pp. 77–86, May 2017.
[3] M. Asikuzzaman, M. J. Alam, A. J. Lambert, and M. R. Pickering, "Robust DT CWT-based DIBR 3D video watermarking using chrominance embedding," *IEEE Trans. Multimedia*, vol. 18, no. 9, pp. 1733–1748, Jul. 2016.
[4] Q. Su, Y. Niu, G. Wang, S. Jia, and J. Yue, "Color image blind watermarking scheme based on QR decomposition," *Signal Process.*, vol. 94, no. 1, pp. 219–235, Jan. 2014.
[5] D. Sharma, R. Saxena, and N. Singh, "Dual domain robust watermarking scheme using random DFRFT and least significant bit technique," *Multimedia Tools Appl.*, vol. 76, no. 3, pp. 3921–3942, Feb. 2017.
[6] C. H. Chou, and T. L. Wu, "Embedding color image watermarks in color images," *EURASIP J. Advances Signal Process.*, no. 1, pp. 32–40, Jan. 2003.
[7] J. varghese, S. subash, O. b. hussain, k. nallaperumal, M. R. saady, and M. S. khan, "An improved digital image watermarking scheme using the discrete fourier transform and singular value decomposition," *Turkish J. Electr. Eng. Comput. Sci.*, vol. 24, no. 5, pp. 3432–3447, Jun. 2016.
[8] M. Cedillo-Hernandez, F. Garcia-Ugalde, M. Nakano-Miyatake, and H. Perez-Meana, "Robust watermarking method in DFT domain for effective management of medical imaging," *Signal, Image Video Process.*, vol. 9, no. 5, pp. 1163–1178, Jul. 2015.
[9] N. Aherrahrou, and H. Tairi, "A new image watermarking technique based on periodic plus smooth decomposition," *Soft Comput.*, vol. 22, no. 7, pp. 2369–2379, Apr. 2018.
[10] M. Urvoy, D. Goudia, and F. Autrusseau, "Perceptual DFT watermarking with improved detection and robustness to geometrical distortions," *IEEE Trans. Inf. Forensics Security*, vol. 9, no. 7, pp. 1108–1119, Jul. 2014.
[11] Q. Su, Y. Niu, Q. Wang, and G. Sheng, "A blind color image watermarking based on dc component in the spatial domain," *Optik-Int. J. Light Electron Opt.*, vol. 124, no. 23, pp. 6255–6260, Dec. 2013.
[12] N. E. H. Golea, R. Seghir, and R. Benzid, "A bind RGB color image watermarking based on singular value decomposition," in *Proc. IEEE, ACS Int. Conf. Comput. Syst. Appl.*, May 2010, pp. 1–5.
[13] Q. Su, Y. Niu, X. Liu, and Y. Zhu, "Embedding color watermarks in color images based on Schur decomposition," *Opt. Commun.*, vol. 285, no. 7, pp. 1792–1802, Apr. 2012.
[14] S. Jia, "A novel blind color images watermarking based on SVD," *Optik-Int. J. Light Electron Opt.*, vol. 125, no. 12, pp. 2868–2874, Jun. 2014.
[15] Q. Su, G. Wang, X. Zhang, G. Lv, and B. Chen, "A new algorithm of blind color image watermarking based on LU decomposition," *Multidimensional Syst. Signal Process.*, vol. 29, no. 3, pp. 1055–1074, Jul. 2018.
[16] W. Song, J. J. Hou, Z. H. Li, and L. Huang, "Chaotic system and qr factorization based robust digital image watermarking algorithm," *J. Central South Univ. Technol.*, vol. 18, no. 1, pp. 116–124, Feb. 2011.
[17] University Granada. *Computer Vision Group. CVG-UGR Image Database*. Accessed: Mar. 13, 2017. [Online]. Available: http://decsai.ugr.es/cvg/dbimagenes/c512.php
[18] University of Southern California. *Signal and Inage Processing Institute. USC-SIPI Image Database*. Accessed: Mar. 15, 2017. [Online]. Available: http://sipi.usc.edu/database/
[19] R. L. Rivest. *The MD5 Message Digest Algorithm*. Internet RFC, Internet FAQ Archives, MIT Lab. Comput. Sci., Cambridge, MA, USA, 1992, p. 1321.
[20] Q. Su, G. Wang, X. Zhang, G. Lv, and B. Chen, "An improved color image watermarking algorithm based on QR decomposition," *Multimedia Tools Appl.*, vol. 76, no. 1, pp. 707–729, Jan. 2017.
[21] Q. Su, and B. Chen, "Robust color image watermarking technique in the spatial domain," *Soft Comput.*, vol. 22, no. 1, pp. 91–106, Jan. 2018.
[22] J. Zou, and X. Tie, "Arnold transformation of digital image with two dimensions and its periodicity," *J. North China Univ. Technol.*, vol. 12, no. 1, pp. 10–14, Mar. 2000.
[23] L. Vinicius, and R. Jordan, "Geometric attacks on image watermarking systems," *IEEE Multimedia.*, vol. 12, no. 3, pp. 68–78, Jul. 2005.
[24] H. Tian, Y. Zhao, R. Ni, L. Qin, and X. Li, "LDFT-based watermarking resilient to local desynchronization attacks," *IEEE Trans. Cybern.*, vol. 43, no. 6, pp. 2190–2201, Dec. 2013.
[25] D. C. Montgomery and G. C. Runger, *Applied Statistics and Probability for Engineers*, 4th ed. New York, NY, USA, Wiley, 2006.
[26] N. M. Makbol, and B. E. Khoo, "A new robust and secure digital image watermarking scheme based on the integer wavelet transform and singular value decomposition," *Digit. Signal Process.*, vol. 33, pp. 134–147, Oct. 2014.

QINGTANG SU received the M.E. degree from the School of Information and Electronic Engineering, Kunming University of Science and Technology, Kunming, China, in 2005, and the Ph.D. degree in control science and engineering from the East China University of Science and Technology, Shanghai, China, in 2013. He is currently an Associate Professor with the School of Information and Electric Engineering, Ludong University, Yantai, China. His research interests include image processing and information security.

DECHENG LIU received the bachelor's degree from the School of Information and Electrical Engineering, Ludong University, Yantai, China, in 2018, where he is currently pursuing the master's degree. His research interests include image processing and information security.

ZIHAN YUAN received the bachelor's degree from the School of Computer Science and Technology, Jining Medical University, Jining, China, in 2018. She is currently pursuing the master's degree with the School of Information and Electrical Engineering, Ludong University, Yantai, China. Her research interests include image processing and information security.

GANG WANG received the master's degree in optical engineering from the University of Electronic Science and Technology of China, in 2004, and the Ph.D. degree in optical engineering from the Nanjing University of Science and Technology, Nanjing, China, in 2007. He is currently a Professor with the Department Information and Electric Engineering, Ludong University, Yantai, China. His research interest includes image processing.

XIAOFENG ZHANG received the master's degree from the Lanzhou University of Technology, in 2005, and the Ph.D. degree from Shandong University, in 2014. He is currently a Lecturer with the School of Information and Electrical Engineering, Ludong University, China. He has published about 30 papers in international journals and conferences. His research interests include medical image segmentation and pattern recognition.

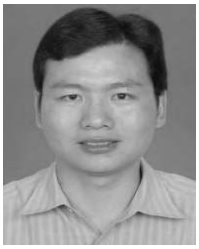

BEIJING CHEN received the Ph.D. degree in computer science from Southeast University, Nanjing, China, in 2011. He is currently an Associate Professor with the School of Computer & Software, Nanjing University of Information Science and Technology, China. His research interests include color image processing, information security, and pattern recognition.

TAO YAO received the M.E. degree from the Wuhan University of Technology, Wuhan, China, in 2006. He is currently an Instructor with the Department Information and Electric Engineering, Ludong University, Yantai, China. His current research interests include digital watermarking and image processing.